Molecular Therapy
Oncolytics
Original Article

Polycytidine tract deletion from microRNA-detargeted oncolytic Mengovirus optimizes the therapeutic index in a murine multiple myeloma model

Velia Penza,[1,3] Justin W. Maroun,[2,3] Rebecca A. Nace,[3] Autumn J. Schulze,[3] and Stephen J. Russell[2,3,4]

[1]Mayo Clinic Graduate School of Biomedical Sciences, Mayo Clinic, Rochester, MN 55902, USA; [2]Mayo Clinic Alix School of Medicine, Mayo Clinic, Rochester, MN 55902, USA; [3]Department of Molecular Medicine, Mayo Clinic, Rochester, MN 55902, USA; [4]Division of Hematology, Mayo Clinic, Rochester, MN, USA

Mengovirus is an oncolytic picornavirus whose broad host range allows for testing in immunocompetent cancer models. Two pathogenicity-ablating approaches, polycytidine (polyC) tract truncation and microRNA (miRNA) targets insertion, eliminated the risk of encephalomyocarditis. To investigate whether a polyC truncated, miRNA-detargeted oncolytic Mengovirus might be boosted, we partially or fully rebuilt the polyC tract into the 5′ noncoding region (NCR) of polyC-deleted (MC_0) oncolytic constructs (NC) carrying miRNA target (miRT) insertions to eliminate cardiac/muscular (miR-133b and miR-208a) and neuronal (miR-124) tropisms. PolyC-reconstituted viruses (MC_{24}-NC and MC_{37}-NC) replicated *in vitro* and showed the expected tropism restrictions, but reduced cytotoxicity and miRT deletions were frequently observed. In the MPC-11 immune competent mouse plasmacytoma model, both intratumoral and systemic administration of MC_0-NC led to faster tumor responses than MC_{24}-NC or MC_{37}-NC, with combined durable complete response rates of 75%, 0.5%, and 30%, respectively. Secondary viremia was higher following MC_0-NC versus MC_{24}-NC or MC_{37}-NC therapy. Sequence analysis of virus progeny from treated mice revealed a high prevalence of miRT sequences loss among MC_{24}- and MC_{37}- viral genomes, but not in MC_0-NC. Overall, MC_0-NC was capable of stably retaining miRT sites and provided a more effective treatment and is therefore our lead Mengovirus candidate for clinical translation.

INTRODUCTION

The generally accepted paradigm for oncolytic viruses (OVs) as cancer therapeutics is that they directly and preferentially lyse infected tumor cells, releasing tumor antigens and creating an immunogenic microenvironment that serves as *in situ* vaccination against the tumor.[1,2] The intrinsic permissiveness of tumor cells for OV infection can be enhanced through modifications to the virus genome that modulate tropism, immunogenicity, and tumor-specific cytotoxicity to achieve an optimal balance of therapeutic safety and potency.[3–5] Mengovirus MC_{24}-NC, an attenuated and microRNA (miRNA)-detargeted picornavirus, was previously shown to be a safe and efficacious OV in a murine multiple myeloma model.[6] However, a consistently curative therapy with complete and durable response across multiple tumor models was not achieved,[7,8] which suggested that the virus may have been over-attenuated and that the therapeutic outcome might be improved if certain attenuating mutations were reversed.

Picornaviruses are single-stranded positive-sense RNA viruses that couple high immunogenicity with rapid replication and high yield of virus progeny. They therefore have the potential to quickly debulk tumors with minimal risk of genotoxicity associated with viral genome integration, and their small particle size allows for efficient extravasation from leaky tumor neovessels.[9] To date, four picornavirus species have been evaluated in phase II clinical trials: a tumor-adapted Enteric cytopathogenic Human Orphan virus 7 (ECHO7 or Rigvir), a porcine pathogen named Seneca Valley virus (SVV), a nonengineered Coxsackievirus (CVA21, or V937), and an engineered poliovirus-human rhinovirus 2 chimera (PVSRIPO).[10–17] As for many other clinically translated OVs, promising preclinical studies showed transient and stable tumor mass reduction, increased survival, responses in non-injected tumors, and acceptable safety profiles. While these findings have been partially replicated in the clinic, complete disease remissions and meaningful therapeutic successes have been inconsistent and sporadic.[18,19]

Mengovirus is a member of the *Cardiovirus* genus and a close relative of encephalomyocarditis virus (EMCV).[20–22] The virus readily infects rodents, which are thought to be the natural reservoir, a variety of other mammalian species including non-human primates such as rhesus monkey and African gray monkey, and is known to infect cell lines derived from a spectrum of human cancers.[6,22–26] In contrast to the strict human cell tropism of other picornaviruses considered for oncolytic virotherapy, such as CVA21 and PVSRIPO, whose preclinical evaluation is restricted to the use of human tumor xenograft

Received 14 September 2022; accepted 29 November 2022;
https://doi.org/10.1016/j.omto.2022.11.006.

Correspondence: Stephen J. Russell, Department of Molecular Medicine, Mayo Clinic, Rochester, MN 55902, USA.
E-mail: sjr@mayo.edu

or transgenic mouse models, Mengovirus can be conveniently studied in immunocompetent mouse tumor models. Because of its species promiscuity, Mengovirus has been studied in immune competent mice, rats, and several other mammals where it has proven to be highly immunogenic and capable of eliciting powerful humoral and cellular cytotoxic responses.[24,25,27–31]

Mengovirus seroprevalence in the human population is low (2%–30%), and infections have been asymptomatic and subclinical.[32–35] Severe symptoms or fatal outcomes have never been reported in humans and a clear correlation between infection and human disease has never been established.[22] In mice and non-human primates, the most common pathologies reported after Mengovirus infection have been pan encephalomyelitis and myocarditis, presenting with flaccid paralysis or sudden death, although the spectrum of symptoms varies greatly depending on route of administration, host adaptation, age, and immunocompetence.[20,22,23,27,36–42] To eliminate the toxicities associated with replication in neuronal and cardiac tissues, our lab created an miRNA-detargeted Mengovirus in which miRNA targeting (miRT) sequences corresponding to miRNAs overexpressed in neuronal (miR-124) and cardiac (miR-133b, miR-208a) tissues were inserted into the 5′ and 3′ non-coding regions (NCR), respectively.[6] miRNA-detargeting successfully controlled virus tropism, restricting its replication to cells and tissues not expressing the cognate miRNAs, thus removing virus-induced toxicity in mice without significantly diminishing oncolytic potency.[6]

Certain viral species in the *Cardiovirus* and *Aphthovirus* genera of the Picornaviridae family contain a polycytidine (polyC) tract 50 to 250 nucleotides long in the 5′ NCR.[43] In Mengovirus, the polyC tract, which occupies a putatively unstructured spacer region between a pseudoknot (pk) and a hairpin structure named stem-loop D, is 55 nucleotides long and contains a single uridine discontinuity, with sequence $C_{44}UC_{10}$.[44] Although the exact function and molecular mechanism by which the polyC tract impacts the virus replication cycle are still to be elucidated for each viral species, several studies have established that the polyC length is a major Mengovirus pathogenicity determinant and that reducing its length proportionally decreases the virulence of the virus *in vivo* without destroying its replication competence.[27,28,45–47] Complete elimination (MC_0) or substantial truncation (MC_{24}, sequence $C_{13}UC_{10}$) of the polyC tract produces live attenuated Mengoviruses capable of establishing infection with absent or very mild symptoms, but nonetheless capable of inducing a powerful immune response that results in long-lasting immunity and protection against re-infection in a variety of mammalian species.[24,25,48–50] Preliminary studies conducted in cultured murine cell lines indicated that the polyC tract might specifically enhance viral replicative fitness in cells of immunological origin.[47]

Here we investigated how increasing the polyC tract length might impact the oncolytic potency of a previously reported polyC truncated, miRNA-detargeted oncolytic Mengovirus (MC_{24}-NC). Our data show that while miRNA-detargeting reliably eliminated virus-related neural and cardiac toxicities irrespective of polyC tract length, the longer polyC tracts were associated with genome instability and these viruses gave rise to a higher frequency of viral progeny with miRNA target sequence deletions. In contrast, the microRNA-detargeted virus with a completely deleted polyC tract (MC_0-NC) proved highly efficacious in an immunocompetent plasmacytoma model, leading to rapid tumor reduction and durable complete response in 75% of mice treated with local or systemic administration combined, without loss of miRT integrity.

RESULTS

PolyC tract length variably affects Mengovirus propagation in different cell types

A direct correlation between polyC tract length and pathogenicity has been established *in vivo*.[27,28,45–47] To further explore the impact of polyC tract length on the ability of Mengovirus to infect and propagate in different cell lineages, we generated non-miRNA-detargeted Mengovirus polyC variants MC_0 (no polyC), MC_{24} ($C_{13}UC_{10}$), and Mwt ($C_{44}UC_{10}$), and tested their replication and cytotoxicity in mouse primary cells (Figure 1A). Primary macrophages (BM-Mφ), dendritic cells (BM-DCs), splenocytes, and adult fibroblasts were isolated from the bone marrow, spleen, and skin of BALB/c mice, respectively. Comparing the cytolytic activity of wild-type Mengovirus (Mwt) across the different primary cell populations showed that fibroblasts are extremely sensitive to the virus showing ∼90% loss of viability by 48 h post-infection, whereas immune cells are relatively resistant, showing only ∼60%–70% loss of viability in macrophages and dendritic cells and an even smaller ∼16% viability loss in infected splenocyte cultures. Viral replication kinetics mirrored these differences in cytotoxicity, resulting in a viral yield five orders of magnitude (in $\log_{10}$) lower in splenocytes than in fibroblasts at an equivalent time point (Figure 1B). Deletion of the polyC tract (MC_0) did not diminish Mengovirus cytotoxicity and/or propagation in fibroblasts but did have a significant impact on the ability of the virus to kill and replicate in macrophages (∼40%), dendritic cells (∼35%), and splenocytes (∼4%) (Figure 1B). These results in primary cells suggest that the long polyC tract in the 5′ NCR of the genome allows Mengovirus to partially overcome a cell-type-specific propagation block present in immune cells, corroborating the observations reported in Martin et al.[45] In order to evaluate whether the cell-type-specific effect of the polyC tract extended to tumor cell lines, a panel of six murine tumor cell lines was selected to cover both non-immunological (4T1, B16-F1, CT26, TC-1) and immunological malignancies (A20 and MPC-11). Susceptibility to Mwt infection varied across cell types (Figure 1C), and the attenuating effect of polyC deletion (MC_0) or truncation (MC_{24}) was most apparent in A20 and MPC-11, the tumor cell lines of immunological origin. Replication kinetics of Mengovirus was also affected by polyC deletion (MC_0), even though the difference with Mwt was not significant (Figure 1C). A similar trend was observed in human tumor cells, where polyC tract length reduction affected cytotoxicity more

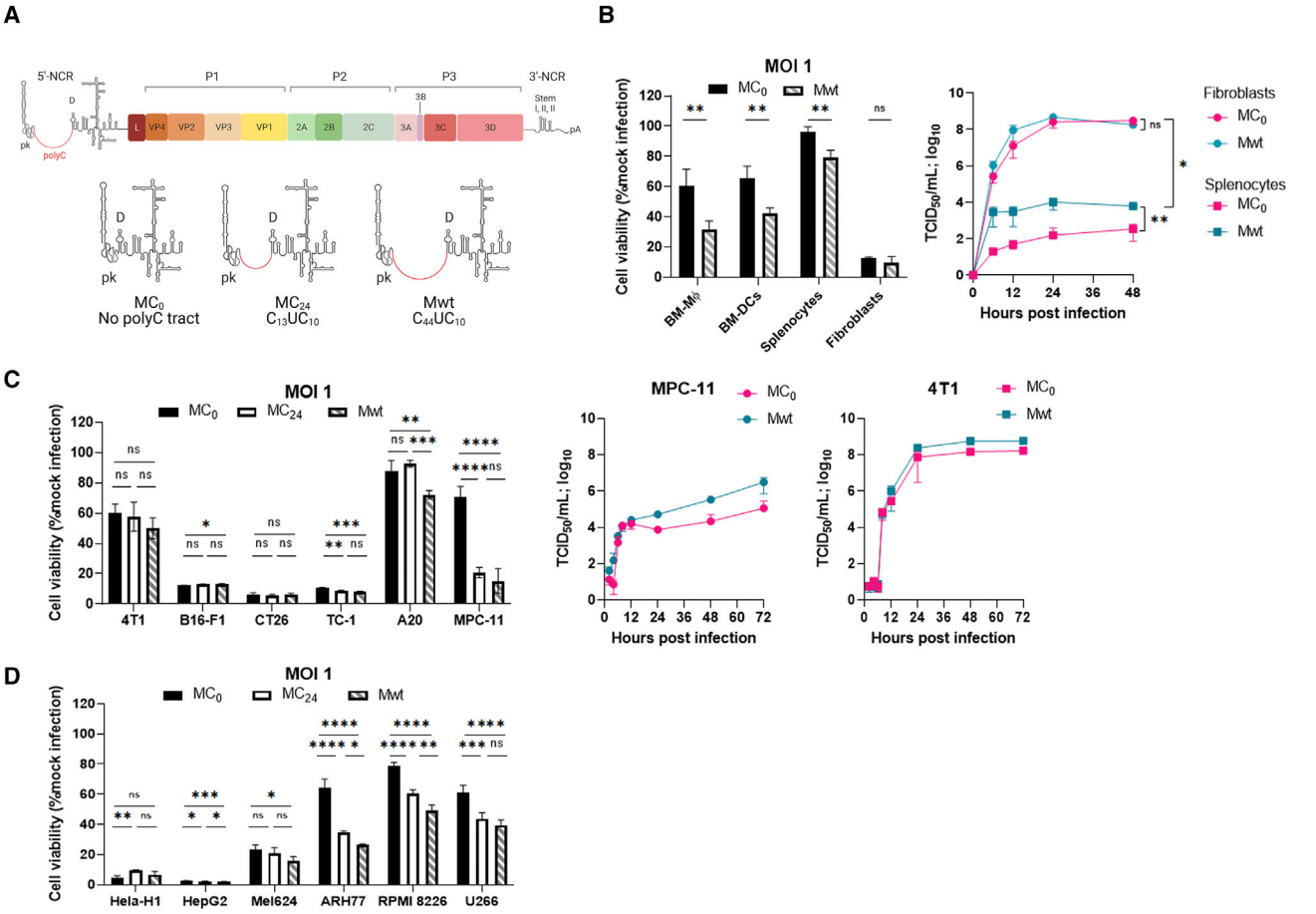

Figure 1. PolyC tract length variably affects Mengovirus propagation in different cell types

(A) Schematic representation of Mengovirus genome: 5′ and 3′ NCRs flanking the coding region (P1-3) with individual genes are shown. Detailed 5′ NCR RNA secondary structures in MC_0 (polyC-deleted), MC_{24} (polyC truncated), and wild type (Mwt) are represented. The polyC positioning between pseudoknot (pk) and stem-loop D is highlighted in red. Based on Carocci and Bakkali-Kassimi,[22] Martin et al.,[45] and Duque and Palmenberg.[51] (B) Propagation of Mengovirus wild-type (Mwt) or the polyC-deleted variant (MC_0) in primary cells isolated/differentiated from BALB/c mice. Bone marrow-derived macrophages (BM-Mφ), bone marrow-derived dendritic cells (BM-DCs), splenocytes, and adult fibroblasts were infected at MOI 1 and cell viability (left) was determined 48 h post-infection through MTT test. Multi-step growth curves (MOI, 0.01) (right) of Mwt and MC_0 in splenocytes and in adult fibroblasts were used to evaluate replication. (C) Viral propagation of Mwt, MC_{24}, or MC_0 in immune (A20 and MPC-11) and non-immune murine tumor cell lines. Cytotoxicity (left) was assessed through MTT assay performed 48 h post-infection at MOI 1. Replication (right) was assessed through multi-step growth curve (MOI, 0.01) of Mwt and MC_0 in non-immunological cell line 4T1 and multiple myeloma cell line MPC-11. (D) Cytotoxicity of Mwt, MC_{24}, or MC_0 (MOI 1) in a panel of immune (ARH77, RPMI 8226, and U266) and non-immune human tumor cell lines, assessed by MTT assay performed 48 h post-infection. Statistical significance was determined through two-tailed t test with Welch's correction in (B); or one-way ANOVA with Tuckey multiple comparison in (C) and (D) (*$p < 0.5$; **$p < 0.01$; ***$p < 0.001$; ****$p < 0.0001$). Data are represented as the average of four technical replicates ± standard deviation. Cartoons created with BioRender.com.

strongly in the B cell-derived cell lines ARH77, RPMI 8226, and U266 (Figure 1D).

Expanding the polyC tract length in miRNA-detargeted Mengoviruses has a negative impact on replicative fitness and is associated with genome instability, but maintains target specificity

To evaluate the impact of combining polyC tract extension with miRNA-detargeting on Mengovirus oncolytic potency, we generated three detargeted viruses with varying polyC tract lengths of 0 (MC_0-NC), 24 (MC_{24}-NC), and 37 (MC_{37}-NC) nucleotides (Figure 2A). Each of these viruses carries two tandem repeats each of three miRT sequences recognized by miRNAs enriched in neuronal (miR-124) and cardiac (miR-133b and miR-208a) tissues. The miR-133b and miR-208a target sequences were inserted into the 3′ NCR upstream of stem loops I–III, and the miR-124 target sequences were inserted into the 5′ NCR, directly upstream of the polyC tract and after the pseudoknot, as previously described.[6] MC_{24}-NC was previously reported to be a safe and relatively potent oncolytic virus, with varying efficacy depending on the tumor model.[6–8] For the purpose of the current study we generated two additional vectors carrying either a full deletion of the polyC tract (MC_0-NC) or a long

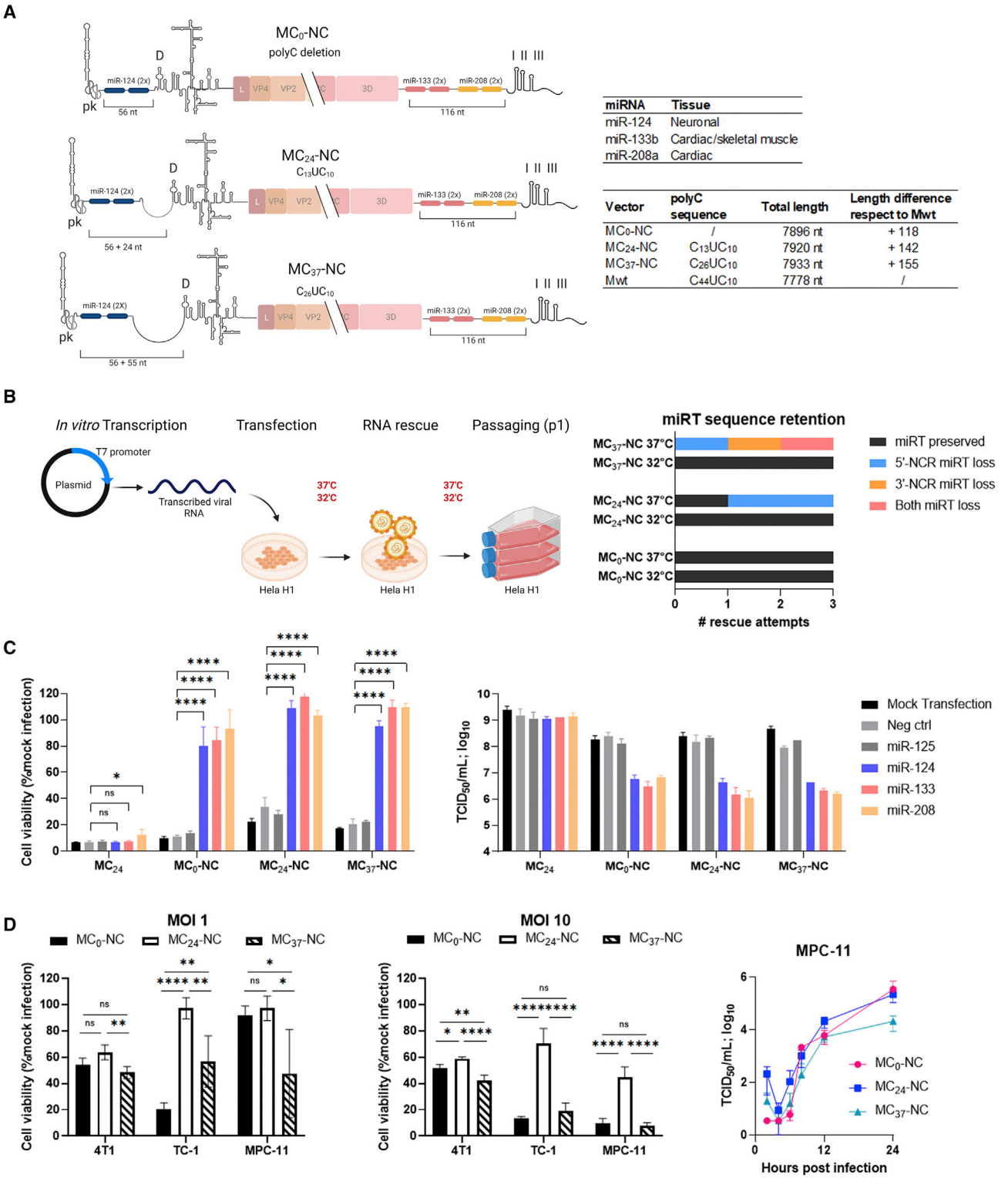

(legend on next page)

polyC tract (MC_{37}-NC) with the sequence $C_{26}UC_{10}$ (Figure 2A). The use of Mengovirus with a wild-type polyC length ($C_{44}UC_{10}$) raises several safety concerns because of its zoonotic potential.[22] Moreover, in attempting to rebuild a full-length 55-residue polyC tract into the miRNA-detargeted Mengovirus genome, technical difficulties with the sequencing of long polyC stretches limited the length of the polyC tract that could be reliably verified post miRT subcloning. However, previous studies on the association between polyC tract length and pathogenicity in Mengovirus have shown that a $C_{26}UC_{10}$ polyC tract has higher virulence than $C_{13}UC_{10}$ (MC_{24}) and approximates the full-length $C_{44}UC_{10}$ polyC in terms of *in vivo* lethality.[45] MC_{37}-NC was therefore used as representative of the long polyC tract.

Combined insertion of the miRT sequences and modulation of the polyC tract length resulted in vector genomes whose length exceeded that of the Mwt genome by 118–155 nucleotides (Figure 2A, table), which was not expected to influence the outcome of our studies since a previous study had shown that Mengovirus genomes with longer insertions could be successfully encapsidated and stably tolerated in Mengovirus vectors.[52] To better maintain insert sequence integrity in the new Mengovirus vectors, virus rescue and amplification were performed at 32°C. Rescue at a higher temperature (37°C) was associated with an increased frequency of insert sequence loss, most notable in the constructs with longer polyC tracts (Figures 2B and S1). This difference suggested that the MC_0-NC genome may be inherently more stable than the MC_{24}-NC and MC_{37}-NC genomes.

We next tested the function of the miRNA-detargeting modifications in all three recombinant viruses using cells transfected with miRNA mimics. As predicted, when synthetic complementary miRNA mimics for miR-124, miR-133b, and miR-208a were transfected in H1-Hela cells 24 h before infection, the replication and cytotoxicity of all three miRNA detargeted variants was significantly reduced, but not in mock transfected cells, nor in cells transfected with an irrelevant miRNA mimic (miR-125 or a *Caenorhabditis elegans* miRNA used as negative control) (Figure 2C).

All three viruses replicated efficiently in the MPC-11 cell line (Figure 2D) and, MC_0-NC cytotoxicity was no different from that of MC_0 in any of the cell lines tested, whereas both MC_{24}-NC and MC_{37}-NC exhibited reduction in cytotoxicity compared with their non-targeted counterparts, and compared with MC_0-NC (Figures 2D and 1C). The loss of cytotoxicity observed for miRNA-detargeted viruses with longer polyC tracts was not directly proportional to the length of their polyC tracts: thus MC_{24}-NC showed diminished cytotoxicity when compared with both MC_0-NC and MC_{37}-NC in the cell lines tested.

miRNA-detargeted polyC-deleted MC_0-NC is associated with more rapid intratumoral replication and superior *in vivo* oncolytic efficacy

Oncolytic activity of the recombinant Mengoviruses was analyzed in BALB/c mice bearing subcutaneous MPC-11 tumors that were previously shown to be responsive to oncolytic Mengovirus therapy.[6] Tumors were established via subcutaneous tumor cell implantation on the right hind flank of BALB/c mice and treated with a single intratumoral (i.t.) dose of 1×10^7 median tissue culture infectious dose ($TCID_{50}$) of MC_0-NC, MC_{24}-NC or MC_{37}-NC. Tumor volume, mouse weight, and overall survival were monitored (Figure 3A, Exp1) and a separate cohort of mice was followed to assess viral replication in the tumors at day 2 and day 6 post-injection (Figure 3A, Exp2).

None of the treated mice developed virus-related toxicities of hindlimb paralysis or myocarditis, confirming that their miRT sequences were functional and prevented toxic replication of the virus in neuronal and cardiac tissues. All mouse deaths in this study were a consequence of tumor progression. Transient weight loss was observed following virus administration but was fully reversible (Figure S2A).

Control mice experienced rapid tumor growth and were euthanized within 10 days of virus administration, excepting one mouse in the i.t.-treated group whose tumor spontaneously regressed post-injection and eventually regrew over the course of 3 weeks (Figure 3B).

All virus-treated mice responded to the therapy, although the magnitude, kinetics, and durability of the responses varied (Figures 3B and 3C, table). Ninety percent of the MC_0-NC-treated mice completely cleared their MPC-11 tumors, with corresponding complete response rates of 10% and 40% for the MC_{24}-NC-treated and MC_{37}-NC-treated groups, respectively. All other treated mice exhibited partial responses, defined as delayed tumor growth or temporary reduction in tumor volume.

Figure 2. MicroRNA-detargeted variants with expanded polyC tracts exhibit miRT instability and reduced replicative fitness but maintain targeting specificity

(A) Schematic representation of miRNA-detargeted Mengovirus polyC variant viruses. Length of the polyC tract, and length and location of the miRT inserts are shown. RNA structural elements highlighted: pseudoknot (pk), stem-loop D (D), and stem-loop I–III. Tables (right) summarize miRT sequences of target tissues and features of the vectors compared with wild-type (Mwt). (B) Rescue protocol and stability of miRT inserts at 32°C versus 37°C. Viruses were rescued in triplicate by RNA transfection and single passage in H1-Hela cells. A summary of the number of rescue attempts that successfully retained the miRT sequences at each temperature is shown on the right, sequencing data shown in Figure S2. (C) Functionality and specificity of microRNA detargeting. H1-Hela cells reverse transfected with cognate miRNA mimics (miR-124, miR-133, miR-208) or negative controls (neg ctrl, miR-125, mock transfection) were infected with miRNA-detargeted viruses or MC_{24} at an MOI of 0.2. Cell viability (left) determined by MTT assay and viral titers (right) were assessed 24 h post-infection. (D) Susceptibility of murine tumor cell lines to miRNA-detargeted infection. Cell viability (left) determined by MTT assay 48 h post-infection at MOI 1 and 10. Multi-step growth curve (MOI 0.01) of miRNA-detargeted viruses in MPC-11. Statistical significance was established through one-way ANOVA with Tuckey multiple comparison in (C) and (D) (*$p < 0.5$; **$p < 0.01$; ***$p < 0.001$; ****$p < 0.0001$). Data are represented as the average of four technical replicates ± standard deviation. Cartoons created with BioRender.com.

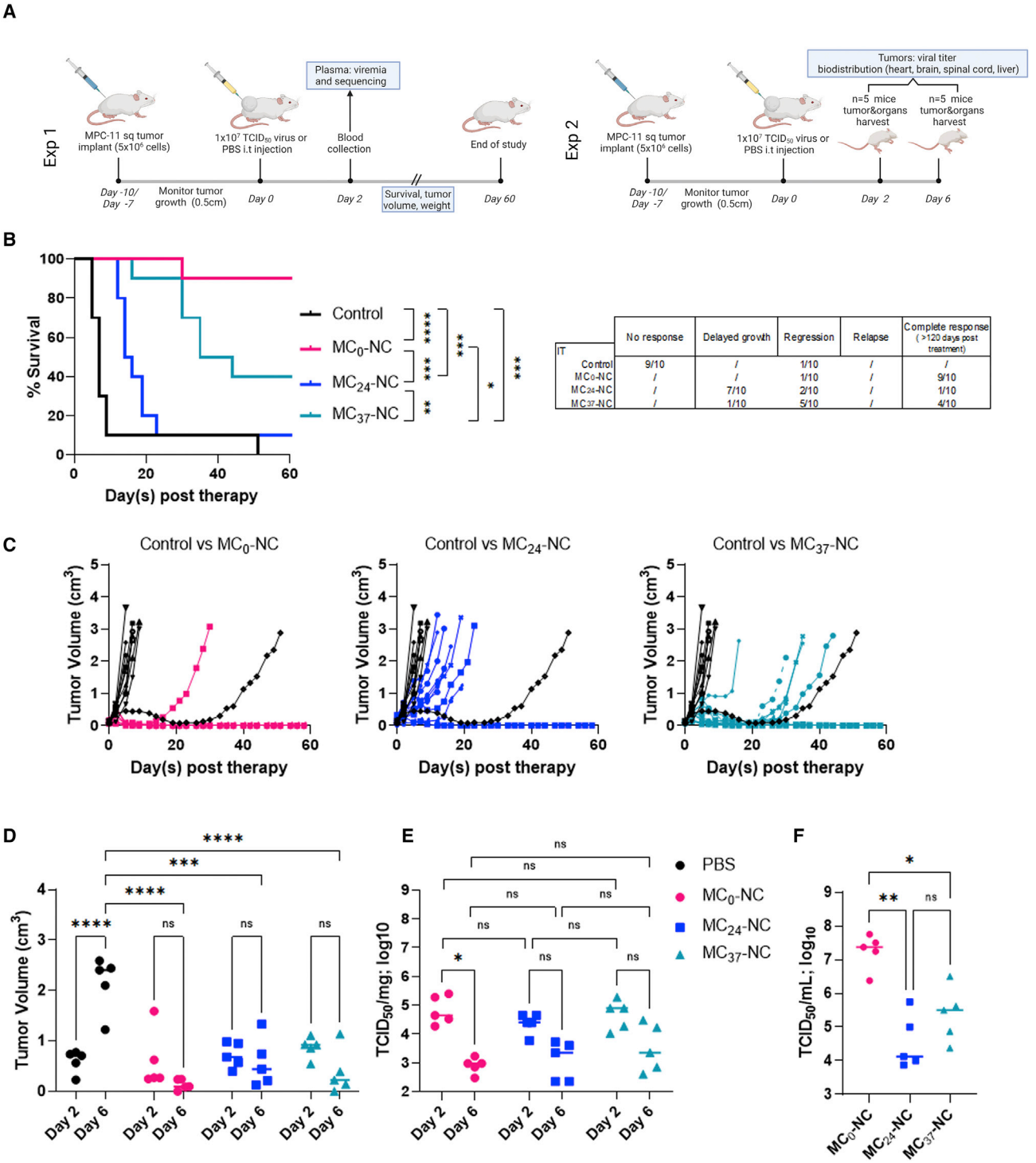

Figure 3. miRNA-detargeted polyC-deleted MC_0-NC is associated with more rapid intratumoral replication and superior *in vivo* oncolytic efficacy

BALB/c mice bearing s.c. MPC-11 tumors were treated with a single intratumoral injection of PBS or 1×10^7 $TCID_{50}$ of MC_0-NC, MC_{24}-NC or MC_{37}-NC, according to the protocol outlined in (A). A second cohort of mice (Exp2) with identical protocol set-up were killed at day 2 and day 6 post-injection to assess viral load in tumors and relevant organs. (B) Overall survival of control PBS-treated (n = 10), MC_0-NC (n = 10), MC_{24}-NC (n = 10), or MC_{37}-NC (n = 10) mice was assessed using Kaplan-Meier survival curves, and statistical significance established through log rank (Mantel-Cox) test (*p < 0.5; **p < 0.01; ***p < 0.001; ****p < 0.0001). Responses to miRNA-detargeted virus therapies are summarized in the table. (C) Disease burden monitored by repeated caliper measurements of tumor volume over time. (D) Tumor regression post miRNA-detargeted virus

(legend continued on next page)

To evaluate intratumoral virus replication and viremic spread to secondary target organs, mice were treated as described (Figure 3A) and were euthanized on days 2 and 6 post-therapy for harvest and analysis of blood, tumor, and selected organs (Figures 3D–3F and S2C). The day 2 intratumoral virus titers show that all three viruses replicated equally efficiently in the tumor milieu, although by day 6 MC_0-NC titers were comparatively lower, perhaps because the tumors treated with this vector were already very small at this time point (Figure 3E).

All three viruses induced high-level viremia, with MC_0-NC reaching significantly higher titers than MC_{37}-NC and MC_{24}-NC (Figure 3F). Recovery of virus from the heart and brain and in trace amounts in the spinal cord at day 2, was likely a reflection of the high viremia in the blood present in said tissues. Virus recovery from nontumor tissues was greatly diminished or absent by day 6 post-injection, which suggests viral clearance was achieved (Figure S2C).

Systemically administered MC_0-NC is also associated with more rapid intratumoral replication and superior *in vivo* oncolytic efficacy

To determine whether polyC tract length could safely impact the antitumor potency of miRNA-detargeted Mengoviruses after systemic administration, which may pose a greater risk of damage to normal cardiac and neural tissue, BALB/c mice bearing syngeneic multiple myeloma MPC-11 tumors were treated with a single intravenous (i.v.) dose of 1×10^7 $TCID_{50}$ of MC_0-NC, MC_{24}-NC, or MC_{37}-NC (Figure 4A).

The only virus-related toxicity observed in these virus-treated animals was temporary weight loss, which resolved spontaneously (Figure S2B). There was no evidence of cardiac or neural toxicity and antitumor activity was comparable to that observed after i.t. administration. While all PBS-treated mice were euthanized within 2 weeks due to rapidly increasing tumor burden, complete tumor responses were observed in 60% of the mice treated with MC_0-NC and 20% of those treated with MC_{37}-NC. Remaining virus-treated mice, including those treated with MC_{24}-NC showed temporary reduction in tumor volume or delayed tumor growth relative to the PBS group (Figures 4B and 4C). As observed following i.t. delivery, day 2 viremia was highest in MC_0-NC treated mice, correlating with the superior antitumor efficacy of this construct.

The MC_0-NC genome shows greater miRT insert stability compared with MC_{24}-NC and MC_{37}-NC genomes

To examine genome stability of the recombinant Mengoviruses, plasma was collected on day 2 post virus administration (i.t. and i.v. routes) from five mice per group and was processed to isolate viral RNA, which was then subjected to 3′ NCR sequencing.

miRT sequences were preserved in all 10 MC_0-NC-treated mice, but point mutations, deletions or recombinations of the entire NCR were detected in approximately half of the mice for each of the MC_{24}-NC and MC_{37}-NC groups (Figure 5A). A 500-nt-long portion of the coding sequence for the viral RNA polymerase (3D gene), which is found proximally to the 3′ NCR, was not affected in any of the three groups, which suggests the genomic instability is limited to the exogenous sequences (Figure 5B). These miRT site alterations appeared in the 3′ NCR, which is not genomically adjacent to the polyC tract itself, suggesting there may be a long-range interaction between the polyC tract in the 5′ NCR and the 3′ NCR that causes loss or destabilization of miRT sequences. Importantly, the appearance of these mutants in the serum of treated animals did not lead to the occurrence of cardiac or neuronal toxicity.

DISCUSSION

In this study, we sought to enhance the potency of an miRNA-detargeted oncolytic Mengovirus by increasing the polyC tract length. We therefore generated three recombinant viral constructs; MC_0-NC (polyC-deleted), MC_{24}-NC (polyC truncated), and MC_{37}-NC (long-tract polyC).

Combining miRT sequence insertion with polyC extension negatively impacted virus efficacy. By rescuing at 32°C, the integrity and functionality of inserted miRT sequences could be preserved and maintained in all three miRNA-detargeted viruses, irrespective of polyC length, but the MC_0-NC design emerged as the most cytotoxic *in vitro*, the most effective *in vivo,* and stably retained its miRT inserts after various viral rescue and amplification protocols as well as during *in vivo* oncolysis.

In a subcutaneous MPC-11 plasmacytoma model in immunocompetent BALB/c mice, a single dose of any one of the three viruses administered i.t. or i.v. significantly impacted tumor volume and survival without causing encephalomyocarditis. However, the depth and duration of tumor responses differed for each of the three viruses and their potency ranking did not correlate directly with polyC length. In both i.t. and i.v. therapy studies, MC_0-NC, with a complete polyC tract deletion, was the most potent of the three; MC_{24}-NC with a 24-residue polyC tract was the least potent, and MC_{37}-NC with an almost fully reconstituted polyC tract, was superior to MC_{24}-NC but less effective than MC_0-NC. Although these findings were counter to original hypotheses, analysis of the genome stabilities of the three viruses showed that the insertion of a polyC tract into an miRNA-detargeted virus genome is associated, during virus replication, with the rapid emergence of variants that have deleted parts of the inserted miRT sequence. This accumulation of deleted genomes was observed both

treatment measured by tumor volume assessed by caliper measurements of tumor volume on day 2 and day 6 post-injection (n = 5 per group, per time point). (E) Viral loads in the tumors of miRNA-detargeted virus-treated mice at day 2 and day 6 post-injection (n = 5 per group, per time point) measured as $TCID_{50}$/mg tissue. Negative results for PBS-treated groups are not shown. (F) Plasma viral loads on day 2 post-injection in miRNA-detargeted virus-treated mice (n = 5 per group) measured as $TCID_{50}$ per mL of plasma. Statistical significance was established through one-way ANOVA with Tukey multiple comparison in (D), (E), and (F) (*$p < 0.5$; **$p < 0.01$; ***$p < 0.001$; ****$p < 0.0001$). Cartoons created with BioRender.com.

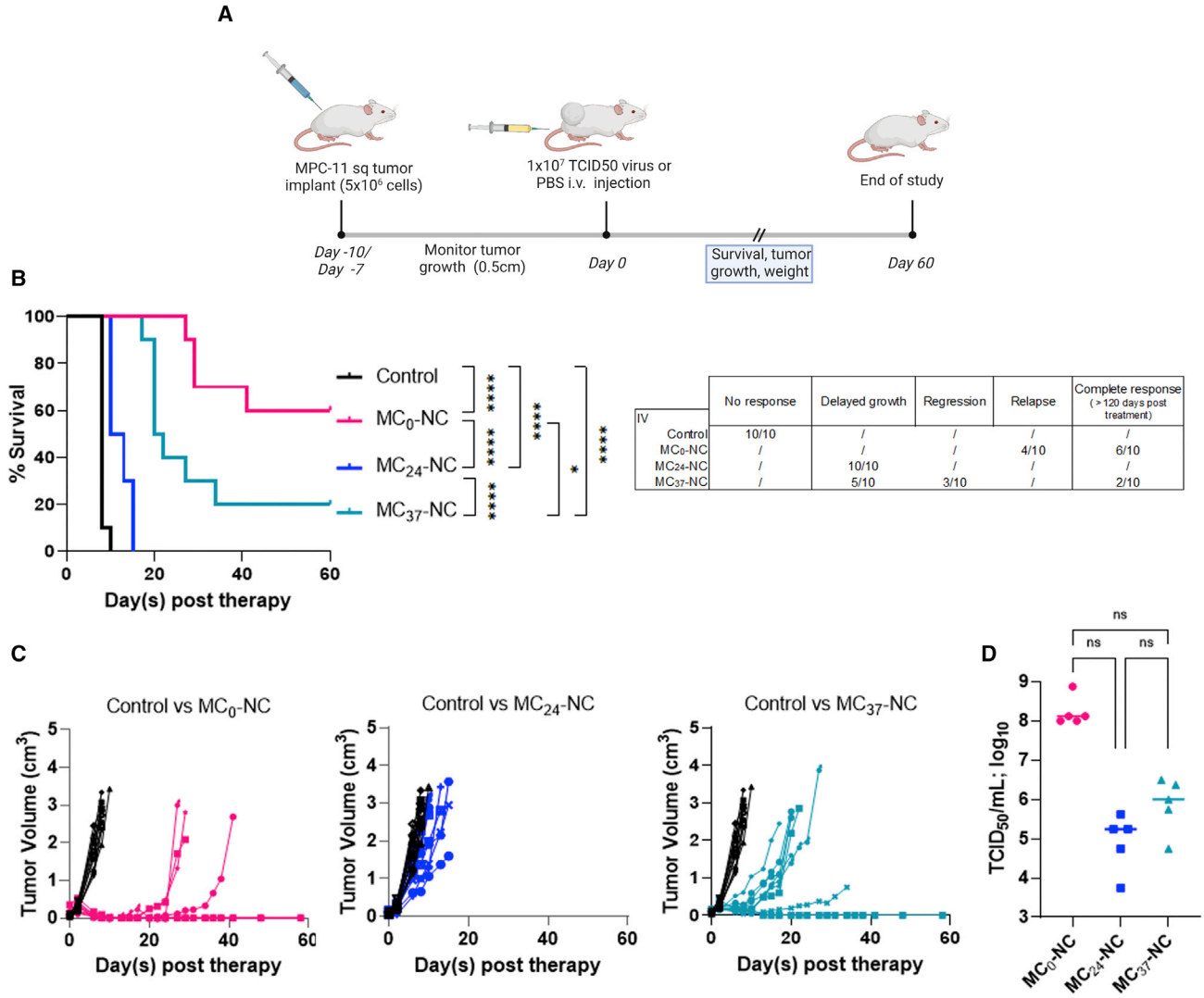

Figure 4. Systemically administered MC0-NC is also associated with more rapid intratumoral replication and superior *in vivo* oncolytic efficacy

BALB/c mice bearing s.c. MPC-11 tumors were treated with a single intravenous injection of PBS or 1 × 107 TCID50 of MC_0-NC, MC_{24}-NC, or MC_{37}-NC, according to the protocol outlined in (A). (B) Overall survival of control PBS-treated (n = 10), MC0-NC (n = 10), MC24-NC (n = 10), or MC37-NC (n = 10) mice assessed using Kaplan-Meier survival curves, and statistical significance established through log rank (Mantel-Cox) test (*p < 0.5; **p < 0.01; ***p < 0.001; ****p < 0.0001). Responses to miRNA-detargeted viruses therapies are summarized in the table. (C) Disease burden monitored by repeated caliper measurements of tumor volume over time. (D) Plasma viral loads on day 2 post-injection in miRNA-detargeted virus-treated mice (n = 5 per group) measured as $TCID_{50}$/mL of plasma. Statistical significance was established through one-way ANOVA with Tukey multiple comparison (*p < 0.5; **p < 0.01; ***p < 0.001; ****p < 0.0001). Cartoons created with BioRender.com.

in vitro during virus amplification on cultured cells, and *in vivo* during intratumoral virus spread.

Because of structural constraints that limit the amount of RNA that can be encapsidated in a picornavirus, the viral genome is under selective pressure to eliminate exogenous sequences that increase its overall size.[53,54] By inserting two copies each of three different miRT sequences into the viruses used in the current study, we added a total of 172 nt to the Mengovirus genome. However, accounting for the polyC tract alterations in each of the three detargeted viruses, their genome lengths diverged from wild type by 118 nt for MC_0-NC, 142 nt for MC_{24}-NC, and 155 nt for MC_{37}-NC. These genome length extensions are small (less than 2% of wild-type genome size) and were therefore potentially tolerable. However, in one previous study that evaluated the tolerability of genome insertions in an attenuated Mengovirus vaccine construct, there was a strong correlation between insert size and loss of infectivity, replication, and genome stability, with a steep reduction in all of these parameters in the 100- to 200-nt range of genome length extension.[52] In keeping with the findings of this published study, loss of miRT insert sequences in the

Figure 5. The MC_0-NC genome shows greater miRT insert stability compared with MC_{24}-NC and MC_{37}-NC genomes

Sequence alignment of the 3′ NCR insertion sites (A) and the RNA polymerase gene (3D) (B) from viral RNA isolated from the plasma of mice treated intratumorally (i.t.) and intravenously (i.v.) with MC_0-NC (mice 11–15), MC_{24}-NC (mice 21–25) and MC_{37}-NC (mice 31–35). A 150-nt-long sub-region of the 3D gene sequence is shown for comparison with the ∼150 miRT insert region (B). Bold red letters represent point mutations and dashed lines represent deletions. Numbering on the reference sequences refers to the nucleotide position with respect to the beginning of the 3′ NCR and 3D gene, to account for the difference in length among the three viruses. Results for miRT sequence retention on 3′ NCR are summarized in the graph (right).

current study was observed more frequently in long polyC tract viruses with total genome lengths that were 142 or 155 nt longer than the wild-type genome, but not for MC_0-NC, which exceeded wt genome length by only 118 nt. Combining miRT insertion with complete polyC deletion may therefore put the MC_0-NC virus below the critical length at which the genome becomes unstable.

A second aspect to consider is the location of the miRT insertions in the genome. The polyC tract and the short region immediately upstream of it in the 5′ NCR, as well as the region upstream of stem loops I–III in the 3′ NCR, do not preferentially form stable secondary or tertiary structures, and insertion in these locations was not expected to alter the surrounding RNA secondary structures.[45,51,] However, it remains possible that alteration of the spacer sequences between the reported secondary structures might disrupt the highly optimized RNA tridimensional arrangement, thereby interfering with replication, translation, packaging, and/or the long-range RNA interactions established between NCRs.[55–57] The total length of the miRT-124 (2X) sequence we inserted upstream of the polyC motif in the 5′ NCR is 56 nt. In the MC_0-NC virus, where the polyC tract (55 nt in Mwt) has been completely removed, the total length of the spacer region between the pseudoknot and stem-loop D is therefore maintained (56 nt), while the MC_{24}-NC and MC_{37}-NC viruses carry longer spacers of 80 nt and 93 nt, respectively. Longer polyC tracts, up to 200 nt in length, have been reported for the closely related cardiovirus, EMCV, suggesting that longer spacer regions may potentially be tolerated in this virus family. However, all Mengovirus isolates analyzed to date have been reported to have polyC spacers in the 50–60-nt range, which indicates that some limitations unique to Mengovirus may need to be taken into consideration.[43] These observations suggest that the highly compact and efficient organization of the picornavirus genome may impose severe constraints that disallow even small variations in the RNA structural landscape. In consequence, the positioning and precise sequence of even small insertions in the Mengovirus genome can have a significant impact on viral fitness, as observed in the current study.

Inherent differences in stability of the viruses reported in this manuscript, caused indirectly by the length of the polyC tract and its relationship to the inserted miRT sequences, may have been further exacerbated by the virus rescue protocol used in the present study. In an effort to preserve the integrity of the inserted miRT sequences during

virus rescue, we lowered the temperature of incubation to 32°C, reduced the number of virus passages, and used high multiplicities of infection (MOI) to generate the viral stocks that were studied. All of these parameters are known to influence the diversity of the viral population, more specifically increasing the frequency of stochastic events that can lead to the generation of defective viral genomes (DVGs), both for Mengovirus and for other RNA viruses.[58–60] Progeny viral particles incorporating DVGs can interfere with the replication of the non-defective genomes either by depleting cellular factors needed for the viral life cycle or by triggering interferon type I-mediated antiviral responses. One additional consideration that we previously reported is that alterations of the RNA secondary structures following miRT site insertions into picornavirus genomes can cause a delay in polyA elongation and consequent reduction in infectivity, and that the polyA length is affected by the temperature used during virus rescue.[56,61] Initial differences in the stability of our recombinant Mengovirus genomes relating to the polyC tract length might therefore have been amplified and/or compounded during virus rescue to result in viral populations more radically impacted in terms of diversity and efficiency of propagation and infection. Notably, MC_0-NC could be easily rescued using conventional and modified protocols without loss of its inserted miRT sequences, which attests to its higher ability to stably retain these foreign sequence elements. Differences in virus populations deriving from the details of the rescue protocols used to generate stocks for *in vivo* evaluation may account for differences between the current study and a previous publication comparing the antitumor activity of different oncolytic Mengoviruses.[6] The impact of OV manufacturing methodology on the efficacy of the final product is an important area for further study.

While the above considerations may account for the superiority of MC_0-NC versus miRNA-detargeted viruses with longer polyC tracts, the reason for the notable lag of MC_{24}-NC replication both *in vitro* and *in vivo* might reside in the fact that the polyC tract $C_{13}UC_{10}$ with a total length of 24 nt is below the threshold length (25–30 nt) previously reported as the necessary minimum to positively impact virus pathogenicity.[45] As discussed above, an underlying instability caused by the longer viral genome might have been further aggravated by the new low temperature rescue protocol used for both MC_{24}-NC and MC_{37}-NC, but it still remains possible that a longer polyC tract combined with a less comprehensive miRT insertion strategy might allow the rescue of a stable oncolytic Mengovirus with superior *in vivo* efficacy and safety profiles.

Harnessing the regulatory power of the miRNA network to control the tropism of viral vectors is a well-established strategy that has been proven feasible in most OV platforms and is particularly effective when applied to viruses with plus sense RNA genomes.[62–72] Picornaviruses are especially suitable for miRNA-detargeting because their mode of entry and cytoplasmic replication exposes the RNA genome to miRT site recognition immediately after uncoating, blocking both viral translation and replication,[73] and has been successfully used to attenuate coxsackieviruses CVA21 and CVB3, poliovirus, and foot-and-mouth disease virus (FMDV).[56,74–78] However, high mutational and recombination rates of picornaviral quasispecies remains an obstacle to insertion of exogenous sequences.[79] Under selective pressure, picornaviruses have been previously reported to lose miRT sequences due to mutations or deletions. Since perfect complementarity is needed for recruitment of the endonuclease into the RNA-induced silencing complex to degrade the target RNA,[63] alterations occasionally generate escape mutants able to evade tissue restriction, causing toxicity, especially in immunocompromised mice.[6,74,78,80] For OV applications specifically, miRNA-detargeting is further challenged by the high titers of virus that must be administered to generate antitumor efficacy and by the fact that the infected tumor becomes a source for sustained generation of progeny genomes, which can potentially saturate the RNAi machinery.[73]

In the current study, symptoms of neurological or cardiac toxicities were not observed following administration of any of the miRNA-detargeted viruses, although mild or sub-lethal damage to normal tissues cannot be excluded. Genomes with deletions and mutations of the miRT sequences were found in the plasma of both MC_{24}-NC and MC_{37}-NC-treated mice as early as 2 days post virus administration; however, full revertants with wild-type virus pathogenicity were not observed. Interestingly, these alterations were limited to the exogenous inserts in the NCR and did not extend to the proximal protein-coding sequence, suggesting a selective pressure against the miRTs. Considering the kinetics with which escape mutants emerge and the kinetics of the antiviral immune response, it can be argued that the escape mutants arrive so late that they are very rapidly controlled by the immune system.

Analysis of virus progeny from MC_0-NC-treated mice identified no mutations or deletions in viral genomes obtained from plasma at day 2 post-injection, the time of peak viremia. However, it remains possible that escape mutants may have been present at low frequency, below the threshold of detection of the methods used. A deeper population-level analysis to quantify and accurately describe population diversity, presence of DVGs, and the types of alterations and their prevalence in body fluids harvested at different timepoints post virus administration could provide more information on this question but was beyond the scope of the current study.

Given the relevance of the polyC tract for Mengovirus replication in immune cells and in tumor cells of immunological origin, it will be fundamental in future studies to address which cells within the tumor microenvironment (TME)—tumor cells, stromal cells, immune cells—are primarily supporting the replication of each of the recombinant Mengoviruses, and whether the viruses are differentially altering the TME composition, particularly with respect to immune cell infiltration and antitumor versus antiviral specific response levels.

Based on the findings reported in the current study, MC_0-NC provides an optimal oncolytic Mengovirus vector design on account of its higher sequence stability, cytotoxicity in tumor cells, and oncolytic activity in an immunocompetent multiple myeloma model. The

combination of attenuation through polyC deletion and tissue restriction via miRNA target insertions also offers remarkable advantages in terms of safety. Deletion of the polyC tract was previously shown to eliminate pathogenicity even at high titers without compromising immunogenicity.[25,27,45] And while miRT insertion may provide only a temporary tropism restriction during the initial stages of *in vivo* replication, polyC deletion constitutes a long-term safety mechanism. The alternative attenuation strategy of polyC truncation to 24 residues in MC_{24} is stably preserved over passaging, but the possibility remains that the polyC tract might eventually be reconstituted through recombination or polymerase slippage, which could potentially lead to the emergence of a fully pathogenic virus under *in vivo* selective pressure. Elongation of a truncated polyC tract has been reported for other viruses, including FMDV, and this mechanism of pathogenicity restoration in MC_{24} Mengoviruses, therefore, remains a concern.[27,44,81,82] In contrast, polyC tract restoration is a less likely outcome after complete deletion of this sequence motif.

Accurately measuring the length of the polyC tract has proven to be a significant technical challenge due to the repetitive nature of the sequence.[43] PolyC deletion may therefore simplify the characterization of a manufactured product for clinical application because it eliminates the need to confirm that the tract length is below the threshold associated with pathogenicity. Also, as reported here, the polyC-deleted virus can be conveniently produced at 37°C.

Overall, our data indicate that restoration of long polyC tracts in oncolytic Mengovirus constructs destabilizes the sequences inserted for genomic miRNA-detargeting and is associated with defective viral propagation and oncolytic activity, even though safety is preserved. Coupling two attenuation strategies—miRNA-detargeting and polyC deletion—produces a highly efficacious oncolytic Mengovirus vector showing an excellent safety profile in the multiple myeloma model that was examined in this study. Future studies will explore the potential of the MC_0-NC virus in a wider spectrum of immunocompetent mouse tumor models and will attempt to unravel the contributions of antitumor immunity and immune cell infection to overall antitumor efficacy.

MATERIALS AND METHODS

Primary cell isolation

Six-week-old female BALB/c mice were purchased from Jackson Laboratories. Mice were euthanized by CO_2 inhalation and death confirmed by cervical dislocation. The skin, spleen, and bone marrow of three donor mice were processed to isolate fibroblasts, splenocytes, macrophages, and dendritic cells.

Primary adult fibroblasts were isolated according to Seluanov et al.[83] Briefly, skin samples were collected from the underarm area, shredded manually with scalpels, and digested for 30 min at 37°C shaking slowly in DMEM/F12 (11320033, ThermoFisher Scientific) media with 0.14 Wunsch U/mL Liberase (5401020001, Roche) and 100 U/mL penicillin–100 µg of streptomycin (15140122, ThermoFisher Scientific). Resulting tissue fragments were washed in complete media DMEM/F12 supplemented with 15% fetal bovine serum, 100 U/mL penicillin–100 µg of streptomycin, twice, and finally resuspended for plating. Tissue fragments were incubated at 37°C, 5% CO_2 until fibroblasts exited the fragments over the course of the next 14 days. Culture media was switched to EMEM supplemented with 15% fetal bovine serum, 100 U/mL penicillin–100 µg of streptomycin, non-essential amino acids in 1:100 dilution (11140050, ThermoFisher Scientific), and 1 mM of sodium pyruvate (11360070, Thermo Scientific) on day 14, after which only adult primary fibroblasts could be used for experiments.

Bone marrow was isolated and differentiated in either macrophages or dendritic cells using a modified protocol from Zhang et al.[84] Briefly, bone marrow was flushed out of long bones (tibias and femurs) of hind legs with ice-cold PBS. Red blood cells were lysed and eliminated with eBioscience RBC Lysis Buffer (00433357, ThermoFisher Scientific) following incubation for 5 min at room temperature. The cells were washed in PBS and resuspended either in macrophage complete media, formulated as DMEM/F12 supplemented with 10% fetal bovine serum, 100 U/mL penicillin–100 µg streptomycin, 100 U/mL M-CSF (315-02 10UG, Peprotech), or dendritic cells complete media, formulated as RPMI 1640 (ThermoFisher Scientific), 10% fetal bovine serum, 100 U/mL penicillin–100 µg of streptomycin, non-essential amino acids in 1:100 dilution and 1 mM of sodium pyruvate, 20 ng/mL GM-CSF (315-03-20UG, Peprotech), and 50 µM β-mercaptoethanol (31350010, ThermoFisher Scientific). On day 3 post isolation, half of the media was removed and replaced with fresh complete media. On day 7 post isolation, bone marrow-derived macrophages and dendritic cells were considered completely differentiated.

Whole spleens were mashed through 70-µm mesh nylon strainers using ice-cold PBS washes and the plunger of a 3-mL syringe. Red blood cells were lysed and eliminated with eBioscience RBC Lysis Buffer following incubation for 5 min at room temperature and the cells washed in PBS. Splenocytes were resuspended in RPMI 1640 supplemented with 10% fetal bovine serum, 100 U/mL penicillin–100 µg of streptomycin, non-essential amino acids, sodium pyruvate, 50 µM β-mercaptoethanol, 10 mM HEPES (15630080, ThermoFisher Scientific) and 50 U/mL interleukin-2 (212-12, Peprotech). For the first 2 days post isolation, complete splenocytes media was supplemented with 2.5 µg/mL concanavalin A. Two days post isolation, splenocytes were considered ready for experiments.

Cell culture

MPC-11 (ATCC, CCL-167) was maintained in DMEM (ThermoFisher Scientific) supplemented with 10% horse serum. A20 (ATCC, TIB-208) was maintained in RPMI 1640 (ThermoFisher Scientific) supplemented with 10% fetal bovine serum and 50 µM β-mercaptoethanol (31350010, ThermoFisher Scientific). HepG2 (ATCC, HB-8065) and Mel264 (ATCC, HTB-71) were maintained in EMEM (ATCC) supplemented with 10% fetal bovine serum; 4T1 (ATCC, CRL-2539), CT26.wt (ATCC, CRL-2638), U266 (ATCC, TIB-196), RPMI 8226 (ATCC, CRM-CCL-155), and ARH77 (ATCC, CRL-1621) were

maintained in RPMI 1640 with 10% fetal bovine serum; B16-F1 (ATCC, CRL-6323), TC-1 (provided by T.C. Wu of Johns Hopkins University), and H1-Hela (ATCC, CRL-1958) were maintained in DMEM supplemented with 10% fetal bovine serum. Cell lines were purchased from and verified by the ATCC (Manassas, VA). All media were supplemented with 100 U/mL penicillin and 100 μg of streptomycin (15140122, Thermo Scientific) and cells incubated in a humidified 37°C incubator with 5% CO_2. ATCC routinely tests morphology, karyotype, and species on cell lines. We performed no further authentication of the cell lines, except on 4T1 cells. Mouse STR profiling and interspecies contamination testing (IDEXX) confirmed mouse origin, genetic profile, and no mammalian interspecies contamination for the 4T1 cells. All cell lines routinely tested negative for mycoplasma contamination.

miRNA-detargeted viruses cloning and rescue

Mengovirus plasmid Rz-pMwt was a kind gift from Ann C. Palmenberg (University of Wisconsin, Department of Biochemistry and the Institute for Molecular Virology), its construction and the construction of pCMV-Rz-Mwt have been described.[6,44,45] Double-stranded DNA (dsDNA) fragments encoding a portion of the 5′ NCR containing a polyC tract of either 0 nt (MC_0), $C_{13}UC_{10}$ (MC_{24}), or $C_{26}UC_{10}$ (MC_{37}) preceded by an additional NheI restriction site (position 148 nt on the wild-type reference sequence for Mengovirus) were synthesized and cloned into pUC57 (GenScript, Piscataway, NJ). The fragments were subcloned into pCMV-Rz-Mwt using EcoRV and AvrII restriction sites. Resulting pMC_0, pMC_{24}, and pMC_{37} were subsequently used as backbones for the cloning of miRNA-detargeted Mengovirus plasmids (pMC_0-NC, pMC_{24}-NC, pMC_{37}-NC), according to the protocol described in Ruiz et al. for pMC_{24}-NC, modified as follows.[6] Briefly, oligonucleotides carrying two tandem copies of miR-124-specific miRT sequences, interspaced by the sequence CGAT and flanked by NheI restriction sites were cloned into the 5′ NCR of the plasmids to obtain the final insert sequence GCTAGCGGCATTCACCGCGTGCCTTACGATGGCATTCACCG CGTGCCTTAGCTAG. The miRT sequences for miR-133b and miRT-208a inserts were already generated for pMC_{24}-NC in Ruiz et al.,[6] and were cloned into pMC_0-NC and pMC_{37}-NC using restriction sites AvrII and EcoRV.

All viruses were rescued as previously described in Ruiz et al.,[6] with the following modifications: RNA transcripts were *in vitro*-transcribed using a MEGAscript T7 Transcription kit (AM1334, ThermoFisher Scientific) and subsequently purified using a MEGAclear Transcription Clean-Up kit (AM1908, ThermoFisher Scientific), both according to the manufacturer's instructions. H1-HeLa cells were seeded into a six-well tissue culture plate at 1×10^6 cells per well; 2.5 μg of purified RNA transcripts were transfected per each well using TransIT-mRNA (MIR2225, Mirus) according to the manufacturer's instructions. Once >70% cytopathic effects (CPE) were observed, cells and supernatants were collected, subjected to three freeze-thaw cycles, debris removed by centrifugation and by 0.22-μm filtration. The entire volume of the viral rescue was used to seed 12 confluent T175 flasks of H1-Hela cells that were harvested following the same protocol to produce passage 1 virus stocks. Cells were incubated at 5% CO_2 either at 32°C or 37°C.

Viral preparations for animal use were concentrated through ultracentrifugation at 28,000× *g* on a 30% sucrose cushion and the pellet resuspended in PBS. Purified virus stocks were tested for endotoxin contamination prior to use in animals.

Integrity of viral sequences was verified by Sanger sequencing as described below, after extracting viral RNA from the preparations using a QIAamp Viral RNA kit (52904, QIAGEN) according to the manufacturer's instructions.

Viral titration

H1-Hela cells were seeded at a concentration of 1×10^4 cells per well in 96-well plates. Ten-fold serial dilutions of virus preparations or clarified tissue lysates were made in Opti-MEM (31985070, ThermoFisher Scientific) and 100 μL of each dilution used to infect each well in eight replicates for each dilution. Virus was allowed to infect for 2 h at 37°C in a 5% CO_2 incubator, then unincorporated virus was removed and fresh complete media added. The plates were incubated at 37°C in 5% CO_2 for 72 h and each well scored positive or negative for CPE. $TCID_{50}$ per mL was calculated using the Spearman and Kärber equation.

Viability assay

The 3-(4,5-dimethylthiazol-2-yl)-2,5-diphenyltetrazolium bromide (MTT) (11465007001, Millipore Sigma) cell proliferation assay was used to measure cytotoxicity in all cell lines; 1×10^4 cells per well were seeded into 96-well plates, viral preparations diluted in Opti-MEM, and infection at indicated MOI was carried out at 37°C in a 5% CO_2 incubator for 2 h. Unincorporated virus was removed and fresh complete media added. Cell viability was determined at 48 h post-infection according to the manufacturer's instructions, and cell viability normalized to mock-infected cells.

Growth curves

Cells were seeded into 12-well plates at a concentration of 2.5×10^5 cells per well. Viruses were diluted in Opti-MEM and cells infected at an MOI of 0.01 for 2 h at 37°C in 5% CO_2. Unincorporated virus was removed and fresh complete media added. At the indicated time points, cells were scraped and collected with the supernatant to be stored at −80°C. Samples were processed simultaneously by three freeze-thawing cycles and centrifugation to eliminate cellular debris. Supernatants were titrated on H1-Hela cells by $TCID_{50}$ as described above.

miRNA assays

miRIDIAN miRNA mimics for miR-124, miR-133b, miR-208a, a miRNA irrelevant for the targeting (miR-125), and a negative control miRNA present in *C. elegans* were purchased from Dharmacon. miRNA mimics were pre-complexed with the TransIR-X2 (MIR6004, MIrus) reagent at a concentration of 200 nM and added to plates prior to H1-Hela seeding, according to the reverse transfection protocol.

Twenty-four hours post transfection, cells were infected with miRNA-detargeted viruses or MC_{24} at an MOI of 0.2. Cell viability assay was performed on 96-well plates with 1×10^4 cells per well and measured through MTT assay as described above, while viral titer was performed on 24-well plates with 2×10^5 cells per well and measured by $TCID_{50}$ on H1-Hela cells, as described above.

Animal experiments

The Mayo Clinic Institutional Animal Care and Use Committee approved all animal studies. Six-week-old female BALB/c mice were purchased from Jackson Laboratories; 5×10^6 washed MPC-11 cells were implanted subcutaneously (s.c.) on the right hind flank. When tumors reached an average diameter of 0.5 cm, mice were treated with 1×10^7 $TCID_{50}$ of MC_0-NC, MC_{24}-NC, or MC_{37}-NC virus diluted in 100 μL PBS, or 100 μL PBS as control, through injection of the tail vein (i.v.) or directly in the tumor (i.t.). Tumor-bearing mice were observed and weighed routinely, and tumor size was measured daily using a caliper. Response to therapy was classified as follows: complete response (tumor elimination lasting over 120 days post treatment), delayed growth (tumor size stabilized, then continues growing), regression (tumor size reduced, then continued growing), or relapse (temporary tumor elimination, then reoccurred). On day 2 post administration, blood was collected from the submandibular vein in MiniCollect Lithium Heparin tubes (450477, Greiner BIO-ONE). Plasma was separated by centrifugation and used to extract viral RNA with the QIAamp Viral RNA kit (52904, QIAGEN) for sequencing.

For the biodistribution study, the same i.t. administration protocol described above was followed. Five animals per group were euthanized on day 2 and day 6 post administration and organs and blood harvested. Tumor, heart, brain, spinal cord, and liver were weighed and homogenized using stainless steel beads (69989, QIAGEN) in a tissue lyser, freeze-thawed three times, and centrifuged; 100 μL of clarified lysates were titrated on H1-Hela as described, and the $TCID_{50}$/mg calculated. Blood was obtained through cardiac puncture at the time of euthanasia, and processed as described above to obtain plasma, 100 μL of which was titrated on H1-Hela and $TCID_{50}$/mL calculated.

Sequencing

Viral RNA extracted from mice sera harvested at day 2 post viral administration in the survival study was sequenced to assess the integrity of miRT sites. cDNA was synthesized using Superscript III first-strand synthesis (18080051, Life Technologies) using oligo-dT as primers, according to the manufacturer's protocol. Noncoding regions containing the miRT sites were amplified using cDNA as template accounting for 1.5% of the total volume of the PCR reaction, using Phusion High-Fidelity DNA polymerase (M0530S, NEB) according to the protocol. The 3′ NCR and partial 3D coding region were amplified using primers GCAGAGGAATTCTTTTCTGAA and CTATTTATTTTACTACTCTAG, while 5′ NCR was amplified using nested PCR with primers GATTGCCGGTCCGCTCGAT ATCG and GGTCTGATAAATTCTCCATCT, followed by primers GGTCCGTGACTACCCACTCC and CCTTCACGACATTCAACA GACC, due to the difficulty of the template. The amplicons were sequenced by Sanger method.

Statistical analysis

GraphPad Prism software, version 8.0.2., was used for data analysis and to assess statistical significance. Viral titer and cell viability were tested using two-tailed t test with Welch's correction or one-way ANOVA with Tuckey multiple comparison as indicated. Kaplan-Meier survival curves were assessed by Mantel-Cox log rank test.

DATA AVAILABILITY

Data are available from the corresponding author upon reasonable request.

SUPPLEMENTAL INFORMATION

Supplemental information can be found online at https://doi.org/10.1016/j.omto.2022.11.006.

ACKNOWLEDGMENTS

The authors thank Sara L. Anderson for the expert secretarial assistance. The authors also thank Ann C. Palmenberg of the University of Wisconsin for the kind gifts of the pF/R-wt and Rz-pMwt plasmids and communications regarding their use, and T.C. Wu of Johns Hopkins University, Department of Gynecologic Pathology for the kind gift of the TC-1 cell line. The authors respect and acknowledge the contribution of Henrietta Lacks and HeLa cells to biomedical research and of all other human tissue donors. V.P. was supported by the Mayo Clinic Graduate School of Biological Science. J.W.M. was supported by the Medical Scientist Training Program at the Mayo Clinic Alix School of Medicine. The present work was funded by the Mayo Clinic Foundation and the National Institutes of Health (NIH) (grants R01CA207386). The graphical abstract for this manuscript was created with Biorender.com.

AUTHOR CONTRIBUTIONS

Conception and design: V.P., A.J.S., and S.J.R. Development of methodology: V.P., J.W.M., A.J.S. Acquisition of data from *in vitro* and *in vivo* experiments: V.P., R.A.N. Analysis and interpretation: V.P., J.W.M., and A.J.S. Writing, review, and revision of the manuscript: V.P., A.J.S., and S.J.R. Study supervision: A.J.S. and S.J.R.

DECLARATION OF INTERESTS

S.J.R. is chief executive officer at Vyriad, an oncolytic virus company. S.J.R. and Mayo Clinic hold equity in Vyriad.

REFERENCES

1. Russell, S.J., and Barber, G.N. (2018). Oncolytic viruses as antigen-agnostic cancer vaccines. Cancer Cell *33*, 599–605. https://doi.org/10.1016/j.ccell.2018.03.011.

2. Melcher, A., Harrington, K., and Vile, R. (2021). Oncolytic virotherapy as immunotherapy. Science *374*, 1325–1326. https://doi.org/10.1126/science.abk3436.

3. Kaufman, H.L., Kohlhapp, F.J., and Zloza, A. (2015). Oncolytic viruses: a new class of immunotherapy drugs. Nat. Rev. Drug Discov. *14*, 642–662. https://doi.org/10.1038/nrd4663.

4. Maroun, J., Muñoz-Alía, M., Ammayappan, A., Schulze, A., Peng, K.W., and Russell, S. (2017). Designing and building oncolytic viruses. Future Virol. *12*, 193–213. https://doi.org/10.2217/fvl-2016-0129.

5. Cattaneo, R., Miest, T., Shashkova, E.V., and Barry, M.A. (2008). Reprogrammed viruses as cancer therapeutics: targeted, armed and shielded. Nat. Rev. Microbiol. *6*, 529–540. https://doi.org/10.1038/nrmicro1927.

6. Ruiz, A.J., Hadac, E.M., Nace, R.A., and Russell, S.J. (2016). MicroRNA-detargeted mengovirus for oncolytic virotherapy. J. Virol. *90*, 4078–4092. https://doi.org/10.1128/JVI.02810-15.

7. Maroun, J.W., Penza, V., Weiskittel, T.M., Schulze, A.J., and Russell, S.J. (2020). Collateral lethal effects of complementary oncolytic viruses. Mol. Ther. Oncolytics *18*, 236–246. https://doi.org/10.1016/j.omto.2020.06.017.

8. Suryawanshi, Y.R., Nace, R.A., Russell, S.J., and Schulze, A.J. (2021). MicroRNA-detargeting proves more effective than leader gene deletion for improving safety of oncolytic Mengovirus in a nude mouse model. Mol. Ther. Oncolytics *23*, 1–13. https://doi.org/10.1016/j.omto.2021.08.011.

9. McCarthy, C., Jayawardena, N., Burga, L.N., and Bostina, M. (2019). Developing picornaviruses for cancer therapy. Cancers (Basel) *11*, 685. https://doi.org/10.3390/cancers11050685.

10. Alberts, P., Tilgase, A., Rasa, A., Bandere, K., and Venskus, D. (2018). The advent of oncolytic virotherapy in oncology: the Rigvir(R) story. Eur. J. Pharmacol. *837*, 117–126. https://doi.org/10.1016/j.ejphar.2018.08.042.

11. Schenk, E.L., Mandrekar, S.J., Dy, G.K., Aubry, M.C., Tan, A.D., Dakhil, S.R., Sachs, B.A., Nieva, J.J., Bertino, E., Lee Hann, C., et al. (2020). A randomized double-blind phase II study of the Seneca Valley virus (NTX-010) versus placebo for patients with extensive-stage SCLC (ES SCLC) who were stable or responding after at least four cycles of platinum-based chemotherapy: north central cancer treatment group (alliance) N0923 study. J. Thorac. Oncol. *15*, 110–119. https://doi.org/10.1016/j.jtho.2019.09.083.

12. Desjardins, A., Gromeier, M., Herndon, J.E., 2nd, Beaubier, N., Bolognesi, D.P., Friedman, A.H., Friedman, H.S., McSherry, F., Muscat, A.M., Nair, S., et al. (2018). Recurrent glioblastoma treated with recombinant poliovirus. N. Engl. J. Med. *379*, 150–161. https://doi.org/10.1056/NEJMoa1716435.

13. Beasley, G.M., Nair, S.K., Farrow, N.E., Landa, K., Selim, M.A., Wiggs, C.A., Jung, S.H., Bigner, D.D., True Kelly, A., Gromeier, M., and Salama, A.K. (2021). Phase I trial of intratumoral PVSRIPO in patients with unresectable, treatment-refractory melanoma. J. Immunother. Cancer *9*, e002203. https://doi.org/10.1136/jitc-2020-002203.

14. Müller, L.M.E., Holmes, M., Michael, J.L., Scott, G.B., West, E.J., Scott, K.J., Parrish, C., Hall, K., Stäble, S., Jennings, V.A., et al. (2019). Plasmacytoid dendritic cells orchestrate innate and adaptive anti-tumor immunity induced by oncolytic coxsackievirus A21. J. Immunother. Cancer *7*, 164. https://doi.org/10.1186/s40425-019-0632-y.

15. Bradley, S., Jakes, A.D., Harrington, K., Pandha, H., Melcher, A., and Errington-Mais, F. (2014). Applications of coxsackievirus A21 in oncology. Oncolytic Virother. *3*, 47–55. https://doi.org/10.2147/OV.S56322.

16. Andtbacka, R.H.I., Curti, B., Daniels, G.A., Hallmeyer, S., Whitman, E.D., Lutzky, J., Spitler, L.E., Zhou, K., Bommareddy, P.K., Grose, M., et al. (2021). Clinical responses of oncolytic coxsackievirus A21 (V937) in patients with unresectable melanoma. J. Clin. Oncol. *39*, 3829–3838. https://doi.org/10.1200/JCO.20.03246.

17. Au, G.G., Lincz, L.F., Enno, A., and Shafren, D.R. (2007). Oncolytic Coxsackievirus A21 as a novel therapy for multiple myeloma. Br. J. Haematol. *137*, 133–141. https://doi.org/10.1111/j.1365-2141.2007.06550.x.

18. Macedo, N., Miller, D.M., Haq, R., and Kaufman, H.L. (2020). Clinical landscape of oncolytic virus research in 2020. J. Immunother. Cancer *8*, e001486. https://doi.org/10.1136/jitc-2020-001486.

19. Martinez-Quintanilla, J., Seah, I., Chua, M., and Shah, K. (2019). Oncolytic viruses: overcoming translational challenges. J. Clin. Invest. *129*, 1407–1418. https://doi.org/10.1172/JCI122287.

20. Dick, G.W.A., Smithburn, K.C., and Haddow, A.J. (1948). Mengo Encephalomyelitis virus: isolation and immunological properties. Br. J. Exp. Pathol. *29*, 547–558.

21. Dick, G.W.A. (1949). The relationship of Mengo Encephalomyelitis, encephalomyocarditis, Columbia-SK and M.M. viruses. J. Immunol. *62*, 11.

22. Carocci, M., and Bakkali-Kassimi, L. (2012). The encephalomyocarditis virus. Virulence *3*, 351–367. https://doi.org/10.4161/viru.20573.

23. Mengo, G.W.A.D. (1948). Encephalomyelitis virus: pathogenicity for animals and physical properties. Br. J. Exp. Pathol. *29*, 18.

24. Osorio, J.E., Hubbard, G.B., Soike, K.F., Girard, M., van der Werf, S., Moulin, J.C., and Palmenberg, A.C. (1996). Protection of non-murine mammals against encephalomyocarditis virus using a genetically engineered Mengo virus. Vaccine *14*, 155–161. https://doi.org/10.1016/0264-410x(95)00129-o.

25. Backues, K.A., Hill, M., Palmenberg, A.C., Miller, C., Soike, K.F., and Aguilar, R. (1999). Genetically engineered Mengo virus vaccination of multiple captive wildlife species. J. Wildl. Dis. *35*, 384–387. https://doi.org/10.7589/0090-3558-35.2.384.

26. Knowles, N.J., Dickinson, N.D., Wilsden, G., Carra, E., Brocchi, E., and De Simone, F. (1998). Molecular analysis of encephalomyocarditis viruses isolated from pigs and rodents in Italy. Virus Res. *57*, 53–62. https://doi.org/10.1016/s0168-1702(98)00081-1.

27. Osorio, J.E., Martin, L.R., and Palmenberg, A.C. (1996). The immunogenic and pathogenic potential of short poly(C) tract Mengo viruses. Virology *223*, 344–350. https://doi.org/10.1006/viro.1996.0485.

28. Duke, G.M., Osorio, J.E., and Palmenberg, A.C. (1990). Attenuation of Mengo virus through genetic engineering of the 5' noncoding poly(C) tract. Nature *343*, 474–476. https://doi.org/10.1038/343474a0.

29. Neal, Z.C., and Splitter, G.A. (1995). Picornavirus-specific CD4+ T lymphocytes possessing cytolytic activity confer protection in the absence of prophylactic antibodies. J. Virol. *69*, 4914–4923.

30. Escriou, N., Leclerc, C., Gerbard, S., Giraud, M., and van der Werf, S. (1995). Cytotoxic T cell response to Mengo virus in mice: effector cell phenotype and target proteins. J. Gen. Virol. *76* (Pt 8), 1999–2007. https://doi.org/10.1099/0022-1317-76-8-1999.

31. Dethlefs, S., Escriou, N., Brahic, M., van der Werf, S., and Larsson-Sciard, E.L. (1997). Theiler's virus and Mengo virus induce cross-reactive cytotoxic T lymphocytes restricted to the same immunodominant VP2 epitope in C57BL/6 mice. J. Virol. *71*, 5361–5365. https://doi.org/10.1128/JVI.71.7.5361-5365.1997.

32. Tesh, R.B. (1978). The prevalence of encephalomyocarditis virus neutralizing antibodies among various human populations. Am. J. Trop. Med. Hyg. *27* (1 Pt 1), 144–149. https://doi.org/10.4269/ajtmh.1978.27.144.

33. Feng, R., Wei, J., Zhang, H., Fan, J., Li, X., Wang, D., Xie, J., Qiao, Z., Li, M., Bai, J., and Ma, Z. (2015). National serosurvey of encephalomyocarditis virus in healthy people and pigs in China. Arch. Virol. *160*, 2957–2964. https://doi.org/10.1007/s00705-015-2591-z.

34. Craighead, J.E., Peralta, P.H., and Shelokov, A. (1963). Demonstration of encephalomyocarditis virus antibody in human serums from Panama. Proc. Soc. Exp. Biol. Med. *114*, 500–503. https://doi.org/10.3181/00379727-114-28714.

35. Oberste, M.S., Gotuzzo, E., Blair, P., Nix, W.A., Ksiazek, T.G., Comer, J.A., Rollin, P., Goldsmith, C.S., Olson, J., and Kochel, T.J. (2009). Human febrile illness caused by encephalomyocarditis virus infection, Peru. Emerg. Infect. Dis. *15*, 640–646. https://doi.org/10.3201/eid1504.081428.

36. Dick, G.W.A., Best, A.M., Haddow, A.J., and Smithburn, K. (1948). Mengo encephalomyelitis; a hitherto unknown virus affecting man. Lancet *2*, 286–289.

37. Psalla, D., Psychas, V., Spyrou, V., Billinis, C., Papaioannou, N., and Vlemmas, I. (2006). Pathogenesis of experimental encephalomyocarditis: a histopathological, immunohistochemical and virological study in mice. J. Comp. Pathol. *135*, 142–145. https://doi.org/10.1016/j.jcpa.2006.04.003.

38. Psalla, D., Psychas, V., Spyrou, V., Billinis, C., Papaioannou, N., and Vlemmas, I. (2006). Pathogenesis of experimental encephalomyocarditis: a histopathological, immunohistochemical and virological study in rats. J. Comp. Pathol. *134*, 30–39. https://doi.org/10.1016/j.jcpa.2005.06.008.

39. Papaioannou, N., Billinis, C., Psychas, V., Papadopoulos, O., and Vlemmas, I. (2003). Pathogenesis of encephalomyocarditis virus (EMCV) infection in piglets during the

viraemia phase: a histopathological, immunohistochemical and virological study. J. Comp. Pathol. *129*, 161–168. https://doi.org/10.1016/s0021-9975(03)00026-4.

40. Zschiesche, W., and Veckenstedt, A. (1979). Pathogenicity of Mengo virus to mice. III. Potentiation of infection by immunosuppressants. Exp. Pathol. *17*, 387–393. https://doi.org/10.1016/s0014-4908(79)80056-3.

41. Guthke, R., Veckenstedt, A., Güttner, J., Stracke, R., and Bergter, F. (1987). Dynamic model of the pathogenesis of Mengo virus infection in mice. Acta Virol. *31*, 307–320.

42. Colter, J.S., Campbell, J.B., and Hatch, L.R. (1965). The pathogenicity of mice of three variants of Mengo encephalomyelitis virus. J. Cell. Physiol. *65*, 229–235. https://doi.org/10.1002/jcp.1030650209.

43. Penza, V., Russell, S.J., and Schulze, A.J. (2021). The long-lasting enigma of polycytidine (polyC) tract. Plos Pathog. *17*, e1009739. https://doi.org/10.1371/journal.ppat.1009739.

44. Duke, G.M., and Palmenberg, A.C. (1989). Cloning and synthesis of infectious cardiovirus RNAs containing short, discrete poly(C) tracts. J. Virol. *63*, 1822–1826.

45. Martin, L.R., Duke, G.M., Osorio, J.E., Hall, D.J., and Palmenberg, A.C. (1996). Mutational analysis of the mengovirus poly(C) tract and surrounding heteropolymeric sequences. J. Virol. *70*, 2027–2031.

46. Osorio, J.E., Grossberg, S.E., and Palmenberg, A.C. (2000). Characterization of genetically engineered mengoviruses in mice. Viral Immunol. *13*, 27–35. https://doi.org/10.1089/vim.2000.13.27.

47. Martin, L.R., Neal, Z.C., McBride, M.S., and Palmenberg, A.C. (2000). Mengovirus and encephalomyocarditis virus poly(C) tract lengths can affect virus growth in murine cell culture. J. Virol. *74*, 3074–3081. https://doi.org/10.1128/jvi.74.7.3074-3081.2000.

48. Altmeyer, R., Escriou, N., Girard, M., Palmenberg, A., and van der Werf, S. (1994). Attenuated Mengo virus as a vector for immunogenic human immunodeficiency virus type 1 glycoprotein 120. Proc. Natl. Acad. Sci. USA *91*, 9775–9779. https://doi.org/10.1073/pnas.91.21.9775.

49. Altmeyer, R., Girard, M., van der Werf, S., Mimic, V., Seigneur, L., and Saron, M.F. (1995). Attenuated Mengo virus: a new vector for live recombinant vaccines. J. Virol. *69*, 3193–3196.

50. Van der Ryst, E., Nakasone, T., Habel, A., Venet, A., Gomard, E., Altmeyer, R., Girard, M., and Borman, A.M. (1998). Study of the immunogenicity of different recombinant Mengo viruses expressing HIV1 and SIV epitopes. Res. Virol. *149*, 5–20. https://doi.org/10.1016/s0923-2516(97)86896-3.

51. Duque, H., and Palmenberg, A.C. (2001). Phenotypic characterization of three phylogenetically conserved stem-loop motifs in the mengovirus 3' untranslated region. J. Virol. *75*, 3111–3120. https://doi.org/10.1128/JVI.75.7.3111-3120.2001.

52. Binder, J.J., Hoffman, M.A., and Palmenberg, A.C. (2003). Genetic stability of attenuated mengovirus vectors with duplicate primary cleavage sequences. Virology *312*, 481–494. https://doi.org/10.1016/s0042-6822(03)00245-9.

53. Mueller, S., and Wimmer, E. (1998). Expression of foreign proteins by poliovirus polyprotein fusion: analysis of genetic stability reveals rapid deletions and formation of cardioviruslike open reading frames. J. Virol. *72*, 20–31. https://doi.org/10.1128/JVI.72.1.20-31.1998.

54. Hammoumi, S., Cruciere, C., Guy, M., Boutrouille, A., Messiaen, S., Lecollinet, S., and Bakkali-Kassimi, L. (2006). Characterization of a recombinant encephalomyocarditis virus expressing the enhanced green fluorescent protein. Arch Virol. Sep *151* (9), 1783–1796. https://doi.org/10.1007/s00705-006-0746-7.

55. Serrano, P., Pulido, M.R., Sáiz, M., and Martínez-Salas, E. (2006). The 3' end of the foot-and-mouth disease virus genome establishes two distinct long-range RNA-RNA interactions with the 5' end region. J. Gen. Virol. *87* (Pt 10), 3013–3022. https://doi.org/10.1099/vir.0.82059-0.

56. Elsedawy, N.B., Nace, R.A., Russell, S.J., and Schulze, A.J. (2020). Oncolytic activity of targeted picornaviruses formulated as synthetic infectious RNA. Mol. Ther. Oncolytics *17*, 484–495. https://doi.org/10.1016/j.omto.2020.05.003.

57. Toyoda, H., Franco, D., Fujita, K., Paul, A.V., and Wimmer, E. (2007). Replication of poliovirus requires binding of the poly(rC) binding protein to the cloverleaf as well as to the adjacent C-rich spacer sequence between the cloverleaf and the internal ribosomal entry site. J. Virol. *81*, 10017–10028. https://doi.org/10.1128/JVI.00516-07.

58. McClure, M.A., Holland, J.J., and Perrault, J. (1980). Generation of defective interfering particles in picornaviruses. Virology *100*, 408–418. https://doi.org/10.1016/0042-6822(80)90532-2.

59. Radloff, R.J., and Young, S.A. (1983). Defective interfering particles of encephalomyocarditis virus. J. Gen. Virol. *64* (Pt 7), 1637–1641. https://doi.org/10.1099/0022-1317-64-7-1637.

60. Vignuzzi, M., and López, C.B. (2019). Defective viral genomes are key drivers of the virus-host interaction. Nat. Microbiol. *4*, 1075–1087. https://doi.org/10.1038/s41564-019-0465-y.

61. Silvestri, L.S., Parilla, J.M., Morasco, B.J., Ogram, S.A., and Flanegan, J.B. (2006). Relationship between poliovirus negative-strand RNA synthesis and the length of the 3' poly(A) tail. Virology *345*, 509–519. https://doi.org/10.1016/j.virol.2005.10.019.

62. Ruiz, A.J., and Russell, S.J. (2015). MicroRNAs and oncolytic viruses. Curr. Opin. Virol. *13*, 40–48. https://doi.org/10.1016/j.coviro.2015.03.007.

63. Bofill-De Ros, X., Rovira-Rigau, M., and Fillat, C. (2017). Implications of MicroRNAs in oncolytic virotherapy. Front. Oncol. *7*, 142. https://doi.org/10.3389/fonc.2017.00142.

64. Ylösmäki, E., Hakkarainen, T., Hemminki, A., Visakorpi, T., Andino, R., and Saksela, K. (2008). Generation of a conditionally replicating adenovirus based on targeted destruction of E1A mRNA by a cell type-specific MicroRNA. J. Virol. *82*, 11009–11015. https://doi.org/10.1128/JVI.01608-08.

65. Lee, C.Y.F., Rennie, P.S., and Jia, W.W.G. (2009). MicroRNA regulation of oncolytic herpes simplex virus-1 for selective killing of prostate cancer cells. Clin. Cancer Res. *15*, 5126–5135. https://doi.org/10.1158/1078-0432.CCR-09-0051.

66. Fu, X., Rivera, A., Tao, L., De Geest, B., and Zhang, X. (2012). Construction of an oncolytic herpes simplex virus that precisely targets hepatocellular carcinoma cells. Mol. Ther. *20*, 339–346. https://doi.org/10.1038/mt.2011.265.

67. Hikichi, M., Kidokoro, M., Haraguchi, T., Iba, H., Shida, H., Tahara, H., and Nakamura, T. (2011). MicroRNA regulation of glycoprotein B5R in oncolytic vaccinia virus reduces viral pathogenicity without impairing its antitumor efficacy. Mol. Ther. *19*, 1107–1115. https://doi.org/10.1038/mt.2011.36.

68. Leber, M.F., Baertsch, M.A., Anker, S.C., Henkel, L., Singh, H.M., Bossow, S., Engeland, C.E., Barkley, R., Hoyler, B., Albert, J., et al. (2018). Enhanced control of oncolytic measles virus using MicroRNA target sites. Mol. Ther. Oncolytics *9*, 30–40. https://doi.org/10.1016/j.omto.2018.04.002.

69. Singh, H.M., Leber, M.F., Bossow, S., Engeland, C.E., Dessila, J., Grossardt, C., Zaoui, K., Bell, J.C., Jäger, D., von Kalle, C., and Ungerechts, G. (2021). MicroRNA-sensitive oncolytic measles virus for chemovirotherapy of pancreatic cancer. Mol. Ther. Oncolytics *21*, 340–355. https://doi.org/10.1016/j.omto.2021.04.015.

70. Rallabandi, R., Sharp, B., Cruz, C., Wang, Q., Locsin, A., Driscoll, C.B., Lee, E., Nelson, T., and Devaux, P. (2022). miRNA-mediated control of exogenous OCT4 during mesenchymal-epithelial transition increases measles vector reprogramming efficiency. Mol. Ther. Methods Clin. Dev. *24*, 48–61. https://doi.org/10.1016/j.omtm.2021.11.012.

71. Edge, R.E., Falls, T.J., Brown, C.W., Lichty, B.D., Atkins, H., and Bell, J.C. (2008). A let-7 MicroRNA-sensitive vesicular stomatitis virus demonstrates tumor-specific replication. Mol. Ther. *16*, 1437–1443. https://doi.org/10.1038/mt.2008.130.

72. Kelly, E.J., Nace, R., Barber, G.N., and Russell, S.J. (2010). Attenuation of vesicular stomatitis virus encephalitis through microRNA targeting. J. Virol. *84*, 1550–1562. https://doi.org/10.1128/JVI.01788-09.

73. Kelly, E.J., Hadac, E.M., Cullen, B.R., and Russell, S.J. (2010). MicroRNA antagonism of the picornaviral life cycle: alternative mechanisms of interference. PLoS Pathog. *6*, e1000820. https://doi.org/10.1371/journal.ppat.1000820.

74. Kelly, E.J., Hadac, E.M., Greiner, S., and Russell, S.J. (2008). Engineering microRNA responsiveness to decrease virus pathogenicity. Nat. Med. *14*, 1278–1283. https://doi.org/10.1038/nm.1776.

75. He, F., Yao, H., Wang, J., Xiao, Z., Xin, L., Liu, Z., Ma, X., Sun, J., Jin, Q., and Liu, Z. (2015). Coxsackievirus B3 engineered to contain microRNA targets for muscle-specific microRNAs displays attenuated cardiotropic virulence in mice. J. Virol. *89*, 908–916. https://doi.org/10.1128/JVI.02933-14.

76. Liu, H., Xue, Y.C., Deng, H., Mohamud, Y., Ng, C.S., Chu, A., Lim, C.J., Lockwood, W.W., Jia, W.W.G., and Luo, H. (2020). MicroRNA modification of coxsackievirus

B3 decreases its toxicity, while retaining oncolytic potency against lung cancer. Mol. Ther. Oncolytics *16*, 207–218. https://doi.org/10.1016/j.omto.2020.01.002.

77. Chang, Y., Dou, Y., Bao, H., Luo, X., Liu, X., Mu, K., Liu, Z., Liu, X., and Cai, X. (2014). Multiple microRNAs targeted to internal ribosome entry site against foot-and-mouth disease virus infection in vitro and in vivo. Virol. J. *11*, 1. https://doi.org/10.1186/1743-422X-11-1.

78. Barnes, D., Kunitomi, M., Vignuzzi, M., Saksela, K., and Andino, R. (2008). Harnessing endogenous miRNAs to control virus tissue tropism as a strategy for developing attenuated virus vaccines. Cell Host Microbe *4*, 239–248. https://doi.org/10.1016/j.chom.2008.08.003.

79. Lauring, A.S., and Andino, R. (2010). Quasispecies theory and the behavior of RNA viruses. PLoS Pathog. *6*, e1001005. https://doi.org/10.1371/journal.ppat.1001005.

80. Gitlin, L., Stone, J.K., and Andino, R. (2005). Poliovirus escape from RNA interference: short interfering RNA-target recognition and implications for therapeutic approaches. J. Virol. *79*, 1027–1035. https://doi.org/10.1128/JVI.79.2.1027-1035.2005.

81. Zibert, A., Maass, G., Strebel, K., Falk, M.M., and Beck, E. (1990). Infectious foot-and-mouth disease virus derived from a cloned full-length cDNA. J. Virol. *64*, 2467–2473.

82. Rieder, E., Bunch, T., Brown, F., and Mason, P.W. (1993). Genetically engineered foot-and-mouth disease viruses with poly(C) tracts of two nucleotides are virulent in mice. J. Virol. *67*, 5139–5145.

83. Seluanov, A., Vaidya, A., and Gorbunova, V. (2010). Establishing primary adult fibroblast cultures from rodents. J. Vis. Exp. 2033. https://doi.org/10.3791/2033.

84. Zhang, X., Goncalves, R., and Mosser, D.M. (2008). The isolation and characterization of murine macrophages. Curr. Protoc. Immunol. Chapter 14, Unit 14.1. https://doi.org/10.1002/0471142735.im1401s83.